



HAL
open science

Combustion instabilities analysis revealed by experimental films using a reduced DMD method

Frédéric Lévy

► **To cite this version:**

Frédéric Lévy. Combustion instabilities analysis revealed by experimental films using a reduced DMD method. 2023. hal-04316279v2

HAL Id: hal-04316279

<https://hal.science/hal-04316279v2>

Preprint submitted on 21 Dec 2023

HAL is a multi-disciplinary open access archive for the deposit and dissemination of scientific research documents, whether they are published or not. The documents may come from teaching and research institutions in France or abroad, or from public or private research centers.

L'archive ouverte pluridisciplinaire **HAL**, est destinée au dépôt et à la diffusion de documents scientifiques de niveau recherche, publiés ou non, émanant des établissements d'enseignement et de recherche français ou étrangers, des laboratoires publics ou privés.

Combustion instabilities analysis revealed by experimental films using a reduced DMD method

Frédéric Lévy

DMPE, ONERA, Université Paris Saclay, F-91123 Palaiseau, France

Two films, realized during a tests campaign on the ONERA Mascotte test bench, were made to study the reactive flow instabilities within a combustion chamber. A camera recorded the chemiluminescence of the OH* radicals and another camera recorded the localization of the liquid phase by shadow imaging. A dynamic mode decomposition code, developed at ONERA, is used to propose another analysis angle of the phenomena recorded by the cameras. The choice was made to reduce all the snapshots of each data set by the mean of the whole sequence. This leads to an analytical solution for the DMD, equivalent to the equations of the discrete Fourier transform. This simple solution allows to process in a quite short time a great amount of data, the limit of which is the computer RAM size. To illustrate the application of this analysis method to a case of experimental results, this paper presents the DMD analysis of the images of both cameras. In fine, the DMD analysis deals with 16001 snapshots for the OH* radicals film, 12281 snapshots for the shadow imaging film, with 524288 values per snapshot.

I. Introduction

IN the In the framework of CNES-ONERA R&D activities for a rocket engine, a test campaign was run on the Mascotte test bench of ONERA, to characterize the atomization process and the combustion regimes, and to supply a database for validation of models and numerical simulation tools. For a matter of confidentiality, no reference is mentioned in this paper about these activities, the results of which are used for DMD only to present an interesting application case with experimental data. The main purpose of the test series, from the point of view of optical diagnostics, was to film the flame using two high-speed cameras which were spatially adjusted (same field viewed by both cameras) and synchronized (images recorded at the same time). A first camera recorded the chemiluminescence of the OH* radicals, which is correlated with the temperature, via an image intensifier. The

second camera was used to visualize the liquid phase by shadow imaging. Both cameras had 1280×800 pixels, with a resolution of 13 pixel/mm. The rough images were cut to the format 1024×512 pixels before being recorded. A shot was selected for the DMD analysis. The films showed a phenomenon of jets and flame pulsation. For this shot, the sampling frequency was 7400 Hz. A narrow band filter was mounted on the UV lens of the OH* camera. This DMD application focuses on the instabilities revealed by two experimental films, dealing 16001 snapshots for the OH* radicals film, 12281 snapshots for the shadow imaging film, with 524288 values per snapshot.

II. Summary of the characteristics of the used DMD method

The equivalence between dynamic mode decomposition and discrete Fourier transform for numerical and experimental data, based on the reduction of all the snapshots by the mean of the whole sequence, was used to propose an analytical and exact solution for the DMD, which is equivalent to the equations for the DFT. The code was developed at ONERA [1]. The sampling time step is assumed to be constant. The time dependant evolution of the modal shapes is a linear combination of all the reduced snapshots, the weight functions being the results of the analytical solution. This solution sets completely free from the constraint to operate matrix processings, which are expensive in time calculation and in memory size if the snapshots number is high. The eigenvalues of the companion matrix are completely independent of the data. They depend only on the snapshots number, and the spectral resolution is uniform. The Nyquist condition is implicitly respected. The tolerance associated with the spectral resolution is half of the resolution frequency. In order to approach the real value of a modal frequency, the tolerance must decrease. Increasing the snapshots number is a convenient possibility, but not the sampling time step, because some information about the researched physical phenomena can be lost. The notion of amplified or damped modes, as it is common in the original DMD analysis, does not exist here, since all the eigenvalues have a unit magnitude. The obtained modes are just preponderant or not, keeping in mind that the notion of modal growth rate is valid only in the time window of the data sequence, since the calculation does not know what happens physically before the first snapshot and after the last one. Whatever the original DMD method can reveal about the dynamical information, it is limited in the time of the observed data. Therefore, it is not unreasonable to turn towards a method, although equivalent to DFT, which presents some other significant advantages, as long as the right preponderant modes of any sequence are still detected. This method is valid regardless of the number and the values of the snapshots. The error of this DMD analysis solution comes only from the data themselves : the time step, the

snapshots number, and the snapshots values. This simple solution allows to process in a quite short time a great amount of data, the limit of which is the computer RAM size. The great advantage of the DMD is the possibility to make visible the time dependant evolution of the shapes of the selected preponderant modes. Dealing with a great number of snapshots allows, in one hand, to compensate some disadvantages outlined for the DFT, and on the other hand, to bring out better the preponderant modes and to make continuous videos of the selected modes shapes. An academic validation case tested at ONERA, typically unsteady and transient, dealing with 50000 snapshots and 125000 values per snapshot, has shown the DMD analysis with the exact analytical solution, equivalent to DFT, works properly to detect the right preponderant modes, under the tolerance frequency.

III. Application to the experimental images

A. Experimental results useful for the DMD analysis

A detailed frequency analysis was made for both films of the selected shot. For all the following images, the fluids move from the left (injectors plane) to the right (downstream). The mean and RMS images were calculated with 5000 images during the steady part of the flow (figure 1 for the OH* radicals images, figure 3 for the shadow images). The projected shadow of the liquid phase is recorded on the retro-lighting images. The figure 2 shows two unsteady OH* radicals images. The diffuse fluid near the injection takes place around the flame from the injector exit. Sometimes, the flame seems to close before the end of the viewing area and shows some puffs. No Abel transform was calculated, because of its questionable physical validity as digital tomography, due to the masking effect of the diffuse fluid.

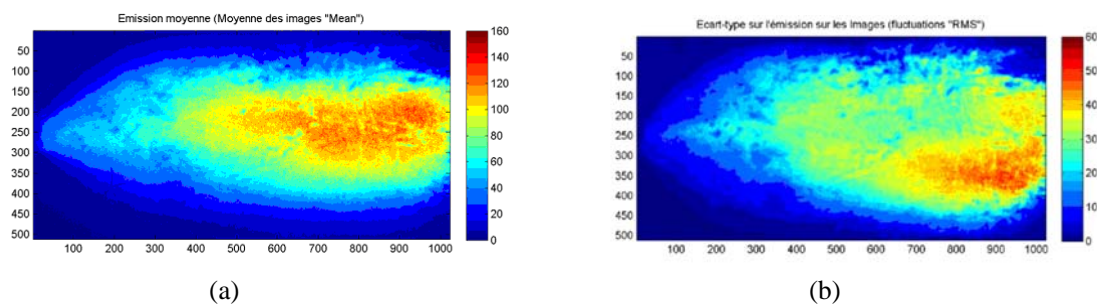


Fig. 1 Mean (a) and RMS (b) OH* images with the narrow band filter

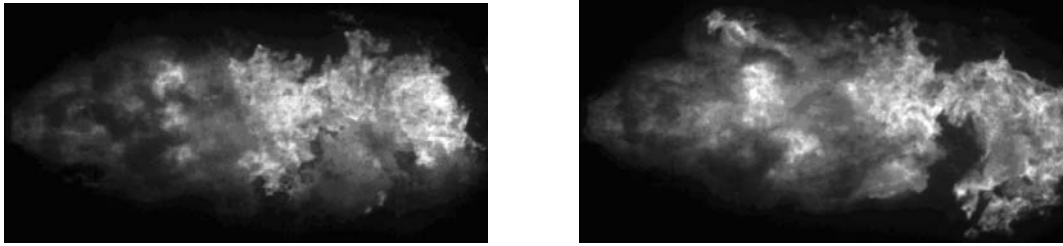


Fig. 2 Unsteady OH* radicals images

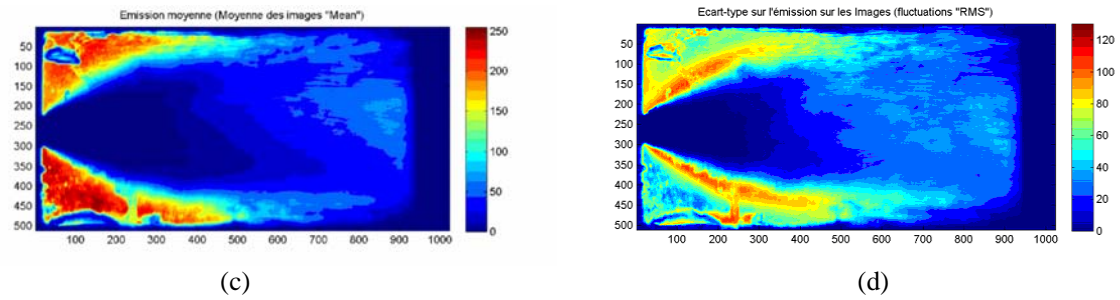


Fig. 3 Mean (c) and RMS (d) shadow images

A first global Fourier analysis was made on the OH* radicals images. Each of them being beforehand spatially averaged, the spectral power density (SPD) of the time dependant resulting signal was then calculated (figure 4). A main peak appears around 2500 Hz. A second very small peak around 3100 Hz seems to come out of the noise.

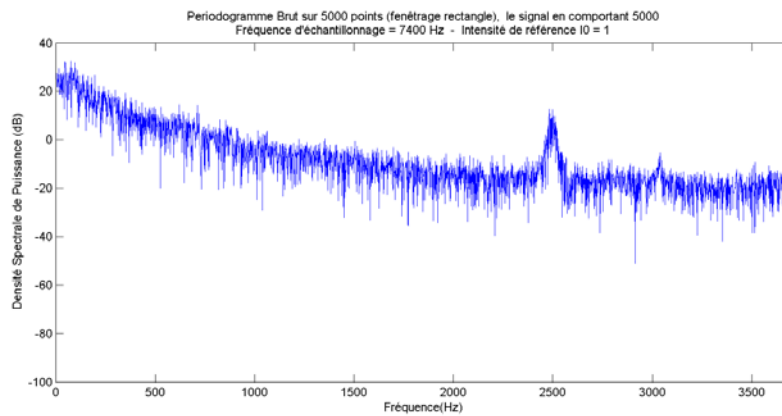


Fig. 4 SPD of the averaged OH* radicals images

The Fourier treatment was then focused on six parts of equal surface in the viewing area. Two other SPD examples, one for the OH* radicals images in a part of the viewing area, and one for the shadow images in

another part, are displayed on the figure 5. In both cases, the obtained SPD shows a little peak at exactly 865 Hz. The peak near 2500 Hz appears only for the OH* images.

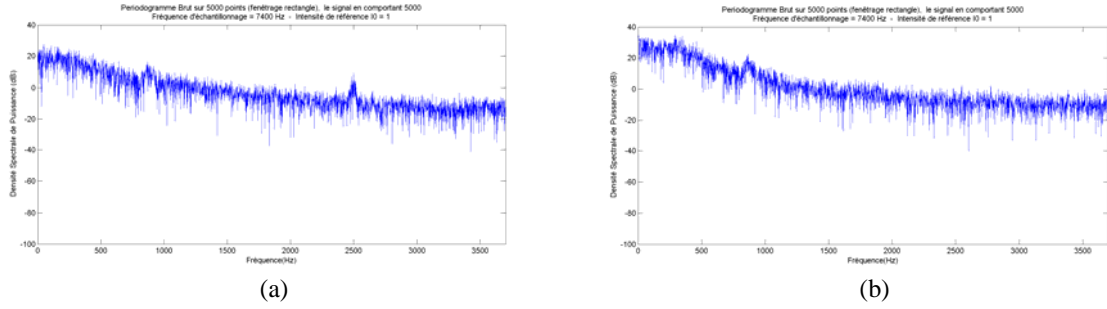


Fig. 5 SPD examples of the OH* radicals images (a), and the shadow images (b) in parts of the viewing area

B. Preponderant modes detected by the DMD analysis for the OH* radicals film

The OH* radicals film was composed of 16001 images, with a sampling frequency of 7400 Hz. Hence the maximum detectable frequency is 3700 Hz and the minimum resolution frequency is 0.4625 Hz, which is very low. Each image has 1024 pixels in abscissa and 512 pixels in ordinate, which makes a total of 524288 values per snapshot, with a spatial resolution of 13 pixel / mm. . To select the preponderant modes, the DMD program calculate the modal amplitudes at $t = 0$. The amplitude of the mode p at the instant j ($t_j = j \Delta t$) is the Euclidean norm of the vector which represents the time dependant evolution of the shape of the mode p . The computer processor contains 24 cores Broadwell Intel® Xeon® CPU E5-2650 v4 @ 2.20GHz, a RAM of 128 GB and a total crest power of 844 GFlops. While running the DMD program, a size of 62.57 Go in the RAM and a total CPU time of 27h 55mn 48s were required to compute the amplitudes of 8000 modes below 3700 Hz at $t = 0$. A specific time can be defined, with a view to estimate the CPU time of other modal amplitudes calculations, including files reading and writing :

$$t_{spec} = \frac{\text{CPU time}}{n_m \times n_s \times n_v} = \frac{100548 \text{ s}}{8000 \times 16001 \times 524288} = 1.498 \cdot 10^{-9} \text{ s} \quad (1)$$

n_m = number of considered modes ;

n_s = snapshots number ;

n_v = values number per snapshot.

The part (a) of the figure 6 shows the modal amplitudes at $t = 0$ of the fluctuations of the pixels grey levels, calculated with all the snapshots, over the whole frequency domain. The selection of the preponderant modes is

made only by visual observation : the amplitude of a preponderant mode is higher than the amplitude of its neighbouring modes. In the case of a DMD analysis from experimental data, the preponderant modes seem to appear like a « bell », in opposition to CFD data where the preponderant modes are very clear at a single frequency. The high value of the sampling time step (near 135 μ s), much higher than the time step in the CFD case (4 μ s), may explain this behaviour, since it leads, with all the snapshots, to a very low resolution frequency. If this frequency is too small, it is then possible that several modes, which provide a similar shape, are captured by several very close frequencies. The amplitude of the phenomenon is then distributed on each of the nearby modes, and it is then difficult to determine a single value of the preponderant mode frequency. If the experimental data comes from an exciting source at a given frequency, then the behaviour associated to the CFD for the DMD analysis is likely to be found again. In this experimental case, the spectrum noise is also quite important, since the images are not filtered.

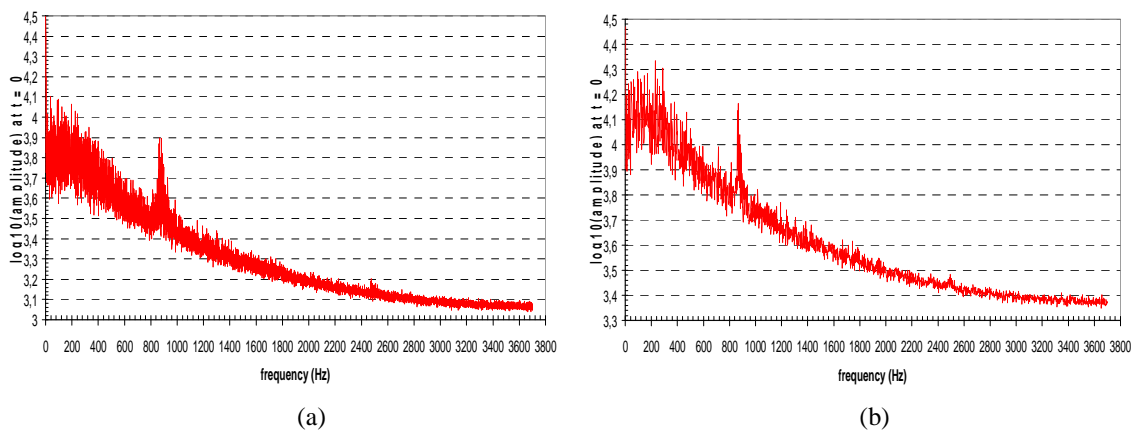


Fig. 6 Modal amplitudes for the OH* radicals film at $t = 0$, with 16001 images (a), and with 3700 images (b)

The part (a) of the figure 6 shows the main phenomenon appears between 850 Hz and 900 Hz. To increase the resolution frequency with a fixed sampling frequency, and therefore, to highlight the preponderant modes at distinct frequencies, it is then required to dim the snapshots number. Then the preponderant mode can be selected more easily. In addition, it is more convenient to choose a snapshots number such as the resolution frequency has a simple value. For the OH* radicals, 3700 continuous snapshots are used (taken here from the 4000th snapshot), and the resolution frequency is 2 Hz. The part (b) of the figure 6 shows the new modal amplitudes at $t = 0$ of the fluctuations of the pixels grey levels. The modal amplitudes as a whole for a reduced number of snapshots are higher than in the case with all the snapshots. Since the sum of all the modal vectors is always equal to the first snapshot regardless of

the snapshots number, it is reasonable to admit, though it is not proved in this paper, that an increasing snapshots number leads overall to a lower amplitude for each modal vector. Four frequencies are selected : 230 Hz, 288 Hz, 866 Hz and 2494 Hz. The preponderant DMD mode for the OH* radicals film appears at 866 Hz (± 1 Hz).

C. Time dependant evolution of the modal shapes for the OH* radicals film

For each selected frequency, a video showing the time dependant evolution of the mode shape can be built. But the modal shapes in this paragraph are shown only at the initial instant (figure 7), because the shapes at further instants do not bring much information. Since the modal shapes are the fluctuations shapes calculated with respect to the rigid mode, the amplitude is positive or negative. The extreme values are reduced compared to the real extreme values of the shapes, in order to highlight better the visible phenomena. The shapes evolutions of the two modes with a high peak at a low frequency (230 Hz and 288 Hz), show a pulsation phenomenon which grows approximately in the middle of the viewing area and moves downstream. It seems to follow the puffing phenomenon of the flame, mentioned in the section A. For the main mode at 866 Hz, the pulsation phenomenon grows from the injection plane before moving downstream and stretching to the upper and lower sides. The waves of the jet mixing zone look conical until about the first third of the viewing area, then they move downstream more longitudinally before they vanish. Since the amplitudes are maximum in the middle of the images, a wavelength λ was measured, along an axial line at $y = 0.2$ m and around the abscissa $x = 0.4$ m. It was found $\lambda = 160$ mm (approximately). A phase velocity can be derived, as the product of λ by the frequency. It is equal to 138.56 m/s. This mode has nothing to do with the acoustics of the chamber, whose first longitudinal mode was calculated at about 611 Hz. The mode at 2494 Hz shows some narrow and swift waves, which take place in the downstream half of the viewing area and which are rather longitudinal.

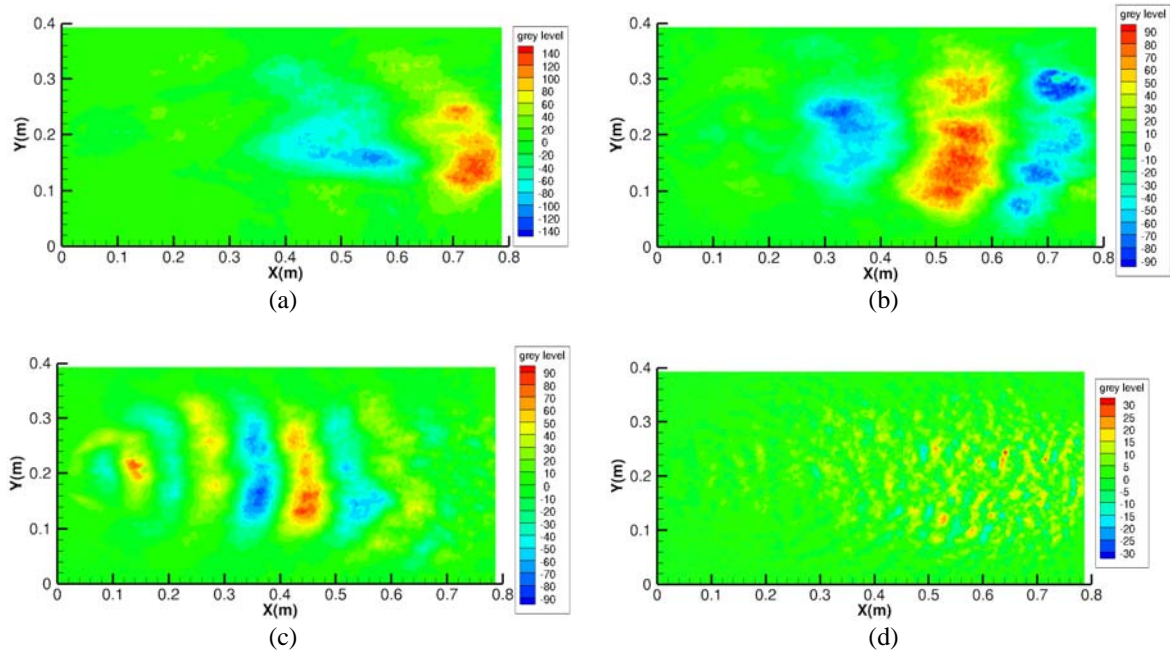


Fig. 7 Modal shapes at $t = 0$ for the OH^* radicals. $f = 230$ Hz (a), $f = 288$ Hz (b), $f = 866$ Hz (c), $f = 2494$ Hz (d)

D. Preponderant modes detected by the DMD analysis for the shadow imaging film

The shadow imaging film was composed of 12281 images, with a sampling frequency of 7400 Hz. The maximum detectable frequency is still 3700 Hz and the minimum resolution frequency is 0.6025 Hz, which is still very low. Each image has still 1024 pixels in abscissa and 512 pixel in ordinate, which makes a total of 524288 values per snapshot, with a spatial resolution of 13 pixel / mm. While running the DMD program, a size of 48.02 Go in the RAM and a total CPU time of 15h 47mn 48s were required to compute the amplitudes of 6140 modes below 3700 Hz at $t = 0$ (the calculations was split up into two parts to respect the maximum allowed CPU time). The specific time, calculated with the relation (1), is here equal to $1.438 \cdot 10^{-9}$ s. The part (a) of the figure 8 shows the modal amplitudes at $t = 0$ of the fluctuations of the pixels grey levels, calculated with all the snapshots, over the whole frequency domain. Again, the preponderant modes seem to appear like a « bell », and the main phenomenon appears between 850 Hz and 900 Hz. The resolution frequency must be increased, to highlight the predominant modes at distinct frequencies. Since the sampling frequency is fixed, the number of snapshots must be reduced. For the shadow images, only 3700 continuous snapshots are used again (taken here from the 4000th snapshot), and the resolution frequency is again 2 Hz. From the part (b) of the figure 8, three modes are selected : 230 Hz, 866 Hz and 1734 Hz. The preponderant DMD mode for the shadow imaging film appears again at 866 Hz (± 1 Hz).

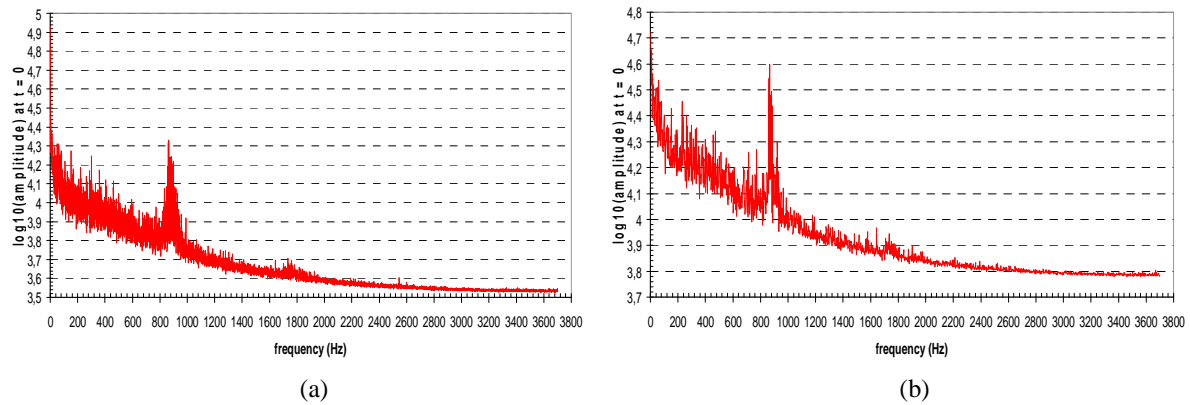


Fig. 8 Modal amplitudes for the shadow images at $t = 0$, with 12281 images (a), and with 3700 images (b)

E. Time dependant evolution of the modal shapes for the shadow imaging film

The time dependant evolution of the selected modes shapes is presented in this paragraph. For each mode, some slides at various moments are extracted from a video which runs over one period of the mode. The shape evolution of the mode at 230 Hz is shown about every next quarter period (figure 9). The time dependant shapes show clearly the separation between the mixing zone of the jet and the recirculation zone between the injector and the walls. The strongest deformations take place along the border around the mixing and burning zone, where the non homogeneities between gas and liquid are the most important.

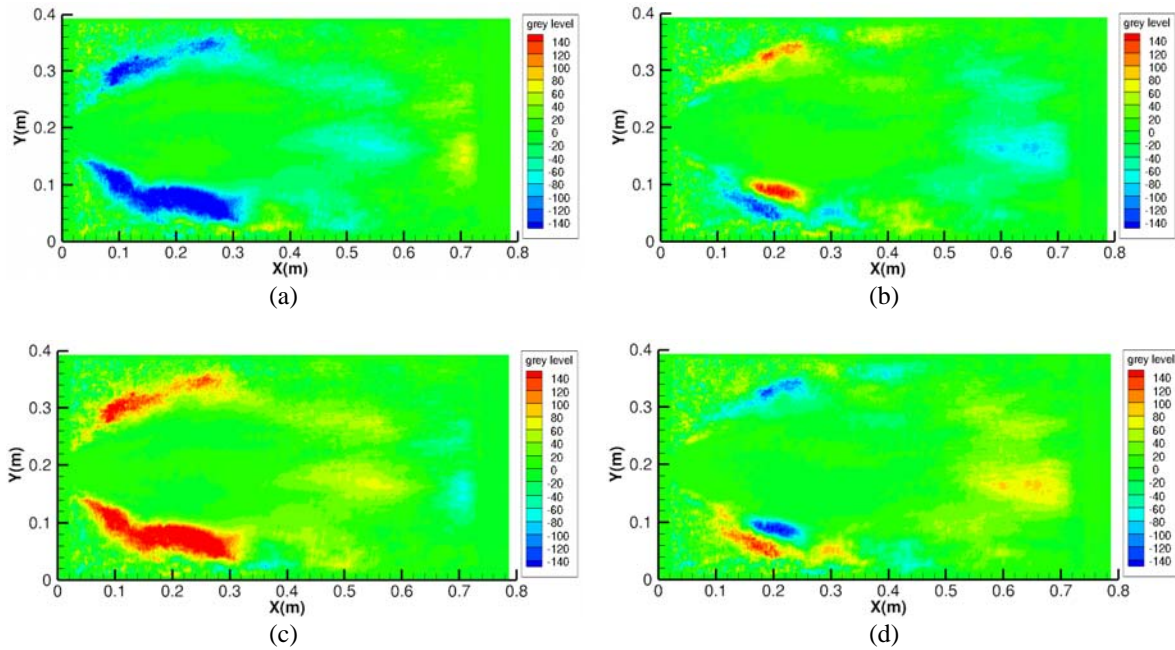


Fig. 9 Shapes of the mode at 230 Hz for the shadow images, at $t = 270 \mu\text{s}$ (a), $t = 1351 \mu\text{s}$ (b), $t = 2432 \mu\text{s}$ (c), $t = 3514 \mu\text{s}$ (d)

The most interesting mode is at 866 Hz. Four moments are shown, from the beginning and every next quarter period (figure 10). These images complement the images of the OH^* radicals pulsations at the same frequency. The pulsations occur essentially along the separation cone between the mixing zone of the jet and the recirculation zone between the injector and the walls. The contrast between liquid and gaseous phases seems to be maximal along this surface, for the considered frequency. It is therefore easy to measure a wavelength, estimated at 196.25 mm, as well as the friction cone opening angle, estimated at 31.67° . The phase velocity in this direction is then equal to 169.95 m/s. The ratio of the OH^* radicals pulsations wavelength to the shadow imaging pulsations wavelength, at the same preponderant mode frequency, is very close to the cosine of the friction cone opening angle. The mode at 1734 Hz seems to be the first harmonic of the previous mode (figure 11). Investigating further the issue about the atomization process, in particular for the preponderant mode, goes beyond the purpose of this paper.

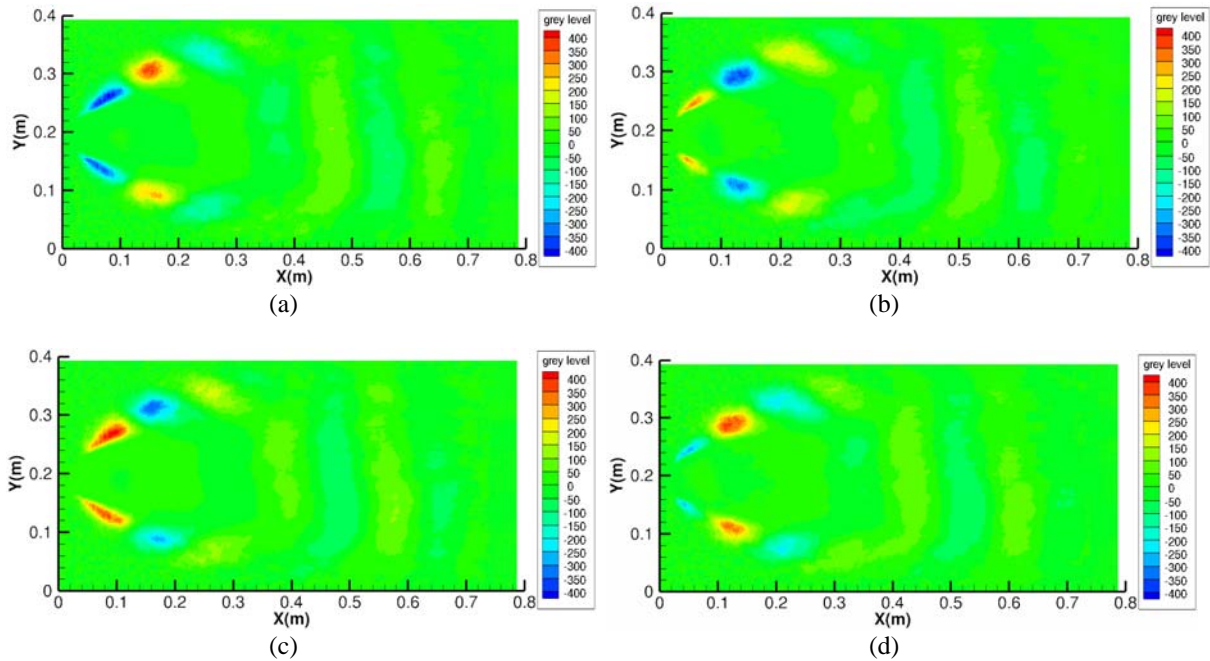


Fig. 10 Shapes of the mode at 866 Hz for the shadow images, at $t = 0$ (a), $t = 405 \mu\text{s}$ (b), $t = 676 \mu\text{s}$ (c), $t = 948 \mu\text{s}$ (d)

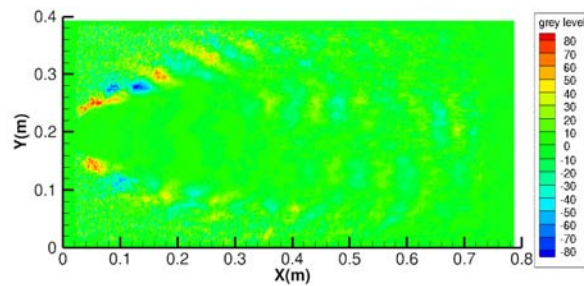


Fig. 11 Shape of the mode at 1734 Hz for the shadow images at $t = 0$

IV. Conclusion

The images of two films, realized during a tests campaign on the Mascotte test bench of ONERA, were used to make a DMD analysis of the combustion instabilities through the chemiluminescence of the OH^* radicals and the localization of the liquid phase by shadow imaging, with the aim to propose another analysis angle of the phenomena recorded by the cameras. For a matter of confidentiality, no reference was mentioned in this paper about these experimental activities. The choice was made to reduce all the snapshots of each data set by the mean of the whole sequence. The subsequent solution for the DMD is then analytic and equivalent to a discrete Fourier

transform. The images of 1024×512 pixels were recorded at 7400 Hz. A spectral power density (SPD) was previously calculated on several parts of equal surface in the viewing area. The results revealed a peak at 865 Hz, for the OH* radicals images and the shadow images, and peak near 2500 Hz only for the OH* images. The DMD analysis, made on the fluctuations of the pixels grey levels, brought out again these frequencies. Appearing initially like a “bell”, due to a too low resolution frequency, the peaks could be isolated by decreasing the number of snapshots, which increased the resolution frequency. For the OH* radicals, 3700 continuous snapshots were used, and the resolution frequency was 2 Hz. A video showing the time dependant evolution of the mode shape was built for each selected frequency. Among four selected frequencies, the main preponderant DMD mode for the OH* radicals film appeared at 866 Hz (± 1 Hz). For this mode, the pulsation phenomenon grew from the injection plane before moving downstream and stretching to the upper and lower sides. The waves of the jet mixing zone looked conical until about the first third of the viewing area, then they moved downstream more longitudinally before they vanished. A wavelength was measured in the middle of the images and a phase velocity was derived. This mode has nothing to do with the acoustics of the chamber, whose first longitudinal mode was calculated at about 611 Hz. For the shadow images, again, only 3700 continuous snapshots were used, and the resolution frequency was 2 Hz. Among three selected frequencies, the main preponderant DMD mode for the shadow imaging film, which appeared again at 866 Hz (± 1 Hz), was the most interesting. The video of the time dependant shapes, which complement the images of the OH* radicals pulsations at the same frequency, showed the pulsations occurred essentially along the separation cone between the mixing zone of the jet and the recirculation zone between the injector and the walls. The contrast between liquid and gaseous phases seemed to be maximal along this surface, for the considered frequency. A wavelength and a friction cone opening angle were measured, and a phase velocity was derived. The ratio of the OH* radicals pulsations wavelength to the shadow imaging pulsations wavelength was very close to the cosine of the friction cone opening angle. Investigating further the issue about the atomization process, in particular for the main preponderant mode, is left to other initiatives.

Acknowledgments

The author wishes to thank Yves Fabignon (ONERA) for encouragement to write this paper, and Nicolas Fdida (ONERA) for providing experimental data as application examples. CNES is gratefully acknowledged for permission to use both experimental films as application data in this paper.

References

- [1] Lévy. F., “Analysis of flows instabilities using a reduced dynamic mode decomposition method, equivalent to a discrete a Fourier transform”, URL : <https://hal.science/hal-03034486> , 2023.